Mitochondrial glutamate acts as a messenger in glucose-induced insulin exocytosis

Maechler, Pierre; Wollheim, Claes

Center). RNAse protection was performed as recommended by the manufacturer (Ambion). Virion-associated RNA used to assess dimerization status was obtained by proteinase K treatment of virions and phenol extraction of purified virus, as described elsewhere[24].

In situ hybridization

Probes were labelled with Cy3 or FITC chromofluors. Cells were fixed with 4% paraformaldehyde and treated as described[25].

Yeast strains and transformation

Wild-type cells containing the reporter constructs were grown for 12–18 h at 30 °C in uracil dropout media with 2% sucrose, and then grown for 6 h in uracil dropout media containing 2% galactose. Cells were spheroplated and viewed by fluorescence microscopy. *Xpo1-1* cells were grown in uracil dropout media with 2% glucose at room temperature and then shifted to 37 °C for 1 h.

Two-hybrid interaction assay

The CRM1 bait construct was provided by M. Rosbash and consists of the whole coding region of CRM1 inserted into pEG202 + PL. Prey constructs were obtained by insertion of wild-type and mutant HIV-1 MA into pJG 4-5. The two-hybrid interaction assay was performed as described[26].

Received 14 September; accepted 1 October 1999.

1. Lewis, P., Hensel, M. & Emerman, M. Human immunodeficiency virus infection of cells arrested in the cell cycle. *EMBO J.* **11,** 3053–3058 (1992).
2. Weinberg, J. B., Matthews, T. J., Cullen, B. R. & Malim, M. H. Productive human immunodeficiency virus type 1 (HIV-1) infection of nonproliferating human monocytes. *J. Exp. Med.* **174,** 1477–1482 (1991).
3. Bukrinksy, M. I. *et al.* Active nuclear import of human immunodeficiency virus type 1 preintegration complexes. *Proc. Natl Acad. Sci. USA* **89,** 6580–6584 (1992).
4. Bukrinsky, M. I. *et al.* A nuclear localization signal within HIV-1 matrix protein that governs infection of non-dividing cells. *Nature* **365,** 666–669 (1993).
5. Bukrinsky, M. I. *et al.* Association of integrase, matrix, and reverse transcriptase antigens of human immunodeficiency virus type 1 with viral nucleic acids following acute infection. *Proc. Natl Acad. Sci. USA* **90,** 6125–6129 (1993).
6. Krausslich, H. G. & Welker, R. Intracellular transport of retroviral capsid components. *Curr. Top. Microbiol. Immunol.* **214,** 25–63 (1996).
7. Fisher, A. G. *et al.* The trans-activator gene of HTLV-III is essential for virus replication. *Nature* **320,** 367–371 (1986).
8. Freed, E. O. HIV-1 gag proteins: diverse functions in the virus life cycle. *Virology* **251,** 1–15 (1998).
9. Clever, J. L. & Parslow, T. G. Mutant human immunodeficiency virus type 1 genomes with defects in RNA dimerization or encapsidation. *J. Virol.* **71,** 3407–3414 (1997).
10. Paillart, J. C. *et al.* A dual role of the putative RNA dimerization initiation site of human immunodeficiency virus type 1 in genomic RNA packaging and proviral DNA synthesis. *J. Virol.* **70,** 8348–8354 (1996).
11. Matthews, S. *et al.* Structural similarity between the p17 matrix protein of HIV-1 and interferon-gamma. *Nature* **370,** 666–668 (1994).
12. Massiah, M. A. *et al.* Three-dimensional structure of the human immunodeficiency virus type 1 matrix protein. *J. Mol. Biol.* **244,** 198–223 (1994).
13. Wolff, B., Sanglier, J. J. & Wang, Y. Leptomycin B is an inhibitor of nuclear export: inhibition of nucleo-cytoplasmic translocation of the human immunodeficiency virus type 1 (HIV-1) Rev protein and Rev-dependent mRNA. *Chem. Biol.* **4,** 139–147 (1997).
14. Nishi, K. *et al.* Leptomycin B targets a regulatory cascade of crm1, a fission yeast nuclear protein, involved in control of higher order chromosome structure and gene expression. *J. Biol. Chem.* **269,** 6320–6324 (1994).
15. Fornerod, M., Ohno, M., Yoshida, M. & Mattaj, I. W. CRM1 is an export receptor for leucine-rich nuclear export signals. *Cells* **90,** 1051–1060 (1997).
16. Fukuda, M. *et al.* CRM1 is responsible for intracellular transport mediated by the nuclear export signal. *Nature* **390,** 308–311 (1997).
17. Ossareh-Nazari, B., Bacheleric, F. & Dargemont, C. Evidence for a role of CRM1 in signal-mediated nuclear protein export. *Science* **278,** 141–144 (1997).
18. Stade, K., Ford, C. S., Guthrie, C. & Weis, K. Exportin 1 (Crm1p) is an essential nuclear export factor. *Cell* **90,** 1041–1050 (1997).
19. Berkowitz, R., Fisher, J. & Goff, S. P. RNA Packaging. *Curr. Top. Microb. Immunol.* **214,** 177–218 (1996).
20. von Schwedler, U., Kornbluth, R. S. & Trono, D. The nuclear localization signal of the matrix protein of human immunodeficiency virus type 1 allows the establishment of infection in macrophages and quiescent T lymphocytes. *Proc. Natl Acad. Sci. USA* **91,** 6992–6996 (1994).
21. Fouchier, R. A., Meyer, B. E., Simon, J. H., Fischer, U. & Malim, M. H. HIV-1 infection of non-dividing cells: evidence that the amino-terminal basic region of the viral matrix protein is important for Gag processing but not for post-entry nuclear import. *EMBO J.* **16,** 4531–4539 (1997).
22. Freed, E. O., Englund, G. & Martin, M. A. Role of the basic domain of human immunodeficiency virus type 1 matrix in macrophage infection. *J. Virol.* **69,** 3949–3954 (1995).
23. Chomczynski, P. A reagent for the single-step simultaneous isolation of RNA, DNA and proteins from cell and tissue samples. *Biotechniques* **15,** 532–534 (1993).
24. Sakuragi, J. I. & Panganiban, A. T. Human immunodeficiency virus type 1 RNA outside the primary encapsidation and dimer linkage region affects RNA dimer stability in vivo. *J. Virol.* **71,** 3250–3254 (1997).
25. Kislauskis, E. H., Zhu, X. & Singer, R. H. Sequences responsible for intracellular localization of beta-actin messenger RNA also affect cell phenotype. *J. Cell Biol.* **127,** 441–451 (1994).
26. Neville, M., Stutz, F., Lee, L., Davis, L. I. & Rosbash, M. The importin-beta family member crm1p bridges the interaction between Rev and the nuclear pore complex during nuclear export. *Curr. Biol.* **7,** 767–775 (1997).

Acknowledgements

We thank J. Mondor, N. Bakker and L. Ross for manuscript preparation. We also thank M. Yoshida for generous donation of Leptomycin B, and M. Rosbash for yeast strains. We thank J. Kan, J. Teodoro, M. Sharkey, J.-M. Jacque, B. Brichacek, S. Swingler and M. Zapp for scientific discussions. This work was supported in part by grants from the NIH to M.R.G. and M.S., and A.B. is supported in part by a Fogarty International Research Collaboration Award. M.R.G. is an investigator of the Howard Hughes Medical Institute.

Correspondence and requests for materials should be addressed to M.R.G. (e-mail: michael.green@umassmed.edu).

Mitochondrial glutamate acts as a messenger in glucose-induced insulin exocytosis

Pierre Maechler & Claes B. Wollheim

Division of Clinical Biochemistry, Department of Internal Medicine, University Medical Centre, 1211 Geneva 4, Switzerland

The hormone insulin is stored in secretory granules and released from the pancreatic β-cells by exocytosis[1]. In the consensus model of glucose-stimulated insulin secretion, ATP is generated by mitochondrial metabolism, promoting closure of ATP-sensitive potassium (K_{ATP}) channels, which depolarizes the plasma membrane[2,3]. Subsequently, opening of voltage-sensitive Ca^{2+} channels increases the cytosolic Ca^{2+} concentration ($[Ca^{2+}]_c$) which constitutes the main trigger initiating insulin exocytosis[1,3,4]. Nevertheless, the Ca^{2+} signal alone is not sufficient for sustained secretion. Furthermore, glucose elicits a secretory response under conditions of clamped, elevated $[Ca^{2+}]_c$ (refs 5, 6). A mitochondrial messenger must therefore exist which is distinct from ATP[7,8]. We have now identified this as glutamate. We show that glucose generates glutamate from β-cell mitochondria. A membrane-permeant glutamate analogue sensitizes the glucose-evoked secretory response, acting downstream of mitochondrial metabolism. In permeabilized cells, under conditions of fixed $[Ca^{2+}]_c$, added glutamate directly stimulates insulin exocytosis, independently of mitochondrial function. Glutamate uptake by the secretory granules is likely to be involved, as inhibitors of vesicular glutamate transport suppress the glutamate-evoked exocytosis. These results demonstrate that glutamate acts as an intracellular messenger that couples glucose metabolism to insulin secretion.

In the β-cell, mitochondria have a pivotal role in the regulation of glucose-induced insulin secretion, and mitochondrial activation is required for normal signal transduction[7–10]. Glucose provides substrates and elevates the Ca^{2+} concentration in the mitochondrial matrix[9] ($[Ca^{2+}]_m$), resulting in further activation of the tricarboxylic-acid (TCA) cycle[10]. We have shown previously that mitochondrial activation generates an unidentified mitochondrial factor, distinct from ATP, which directly triggers insulin exocytosis[7]. We screened molecules derived from mitochondrial metabolism for their secretagogue activity in permeabilized β-cells as described previously[7]. This screening suggested glutamate as a candidate for the putative messenger. Glutamate is formed in the mitochondria from α-ketoglutarate, a TCA-cycle intermediate, by glutamate dehydrogenase[11].

When we incubated rat insulinoma INS-1 cells in the presence of a stimulatory glucose concentration (12.8 mM), cellular glutamate levels increased 4.8-fold within 30 min (Fig. 1a). The stimulated values correspond to a total intracellular glutamate concentration of

approximately 0.22 mM, assuming 200 μg protein per μl cell water (corresponding to 10^6 INS-1 cells). In isolated human pancreatic islets[12], glucose (16.7 mM) also augmented glutamate levels from 0.78 ± 0.65 to 3.93 ± 0.04 nmol per mg protein ($P < 0.025$, $n = 4$) during 30 min incubation. The mitochondrial poison FCCP (carbonyl cyanide *p*-trifluoromethoxyphenylhydrazone) inhibited the production of glutamate during glucose stimulation of INS-1 cells (–43% of cellular glutamate; $n = 5$, $P < 0.01$).

Next we investigated the effects on insulin secretion of a glutamate precursor that was permeable to the cell membrane. Dimethylglutamate (5 mM) caused a leftward shift in the concentration dependency of glucose-stimulated insulin secretion in INS-1 cells (Fig. 1b), in good agreement with observations in rat pancreatic islets[13]. Insulin secretion was not stimulated by dimethylglutamate at basal glucose concentrations or enhanced at optimal glucose concentrations, while secretion was strongly potentiated at intermediate sugar levels. Glutamate is thus formed by mitochondrial metabolism during glucose stimulation (Fig. 1a) and participates in the secretory response (Fig. 1b). These results are consistent with a role for glutamate, derived from glucose, acting downstream of the mitochondria on insulin exocytosis. Accordingly, glutamate dehydrogenase favours glutamate formation rather than providing substrate for the TCA cycle[11,13] during glucose stimulation of the β-cell. This notion is substantiated by the lack of effect of dimethylglutamate on mitochondrial membrane potential ($\Delta\Psi_m$) (reflecting activation of the respiratory chain[10]), measured as the quenching of rhodamine-123 fluorescence (Fig. 2a). Furthermore, dimethylglutamate did not increase $[Ca^{2+}]_m$ in INS-1 cells expressing the Ca^{2+}-sensitive photoprotein aequorin in the mitochondria[9] (Fig. 2b). By contrast, stimulation with methyl succinate, a cell-membrane-permeant precursor for succinate, a TCA cycle intermediate[7], confirms that changes in $\Delta\Psi_m$ and $[Ca^{2+}]_m$ indeed reflect activation of mitochondrial respiration[10] (Fig. 2a, b). Glucose and methyl succinate, both insulin secretagogues, initially increased $[Ca^{2+}]_c$ and hyperpolarized $\Delta\Psi_m$, resulting in a large increase in $[Ca^{2+}]_m$ (refs 7, 9, 14). Therefore, glucose and methyl succinate stimulate insulin secretion by activating mitochondrial metabolism[7,9,14], whereas the metabolic product glutamate apparently participates directly in the secretory process downstream of mitochondrial activation.

To investigate the putative messenger function of glutamate further, we used INS-1 cells permeabilized with *Staphylococcus* α-toxin; in this preparation, insulin secretion in response to mitochondrial substrates is preserved at permissive $[Ca^{2+}]_c$ (ref. 7). Succinate (1 mM), but not glutamate (1 mM), hyperpolarized the $\Delta\Psi_m$ (Fig. 2c). This hyperpolarization facilitated Ca^{2+} uptake by the mitochondria above a threshold of $[Ca^{2+}]_c$ (≈300 nM)[10]. At clamped $[Ca^{2+}]_c$ (500 nM), succinate induced a rise in $[Ca^{2+}]_m$ (Fig. 2d, thick line). This was not observed at 100 nM $[Ca^{2+}]_c$ (Fig. 2d, thin line), a concentration corresponding to basal $[Ca^{2+}]_c$ in intact cells[9]. In contrast to succinate, glutamate did not activate the mitochondria as monitored by $\Delta\Psi_m$ and $[Ca^{2+}]_m$ (Fig. 2c, d).

We next measured insulin secretion in the effluent of permeabilized cells perifused with 1 mM ATP and 500 nM $[Ca^{2+}]_c$. Insulin secretion was stimulated by 1 mM succinate (Fig. 3a), which activated the mitochondrial metabolism by providing substrate and increasing $[Ca^{2+}]_m$ (Fig. 2d). Despite the absence of a rise in $[Ca^{2+}]_m$, glutamate (1 mM) increased insulin secretion from 0.47 ± 0.08 to 1.09 ± 0.25 ng per min ($P < 0.05$, $n = 7$) (Fig. 3b), that is, to the same extent as succinate. At 0.1 mM, glutamate still slightly augmented insulin release, from 0.53 ± 0.03 to 0.84 ± 0.13 ng per min ($P < 0.05$, $n = 4$), but 0.02 mM glutamate was ineffective (data not shown). This concentration range agrees well with the glutamate levels we found in glucose-stimulated INS-1 cells (0.22 mM following 30 min incubation; see above).

Succinate-induced insulin secretion requires the associated rise in $[Ca^{2+}]_m$ for the generation of a messenger[7,8]. We propose that the messenger is glutamate because this molecule was able to trigger exocytosis without mitochondrial activation at 500 nM $[Ca^{2+}]_c$ (Fig. 3b). Nevertheless, an elevated Ca^{2+} concentration in the cytosol

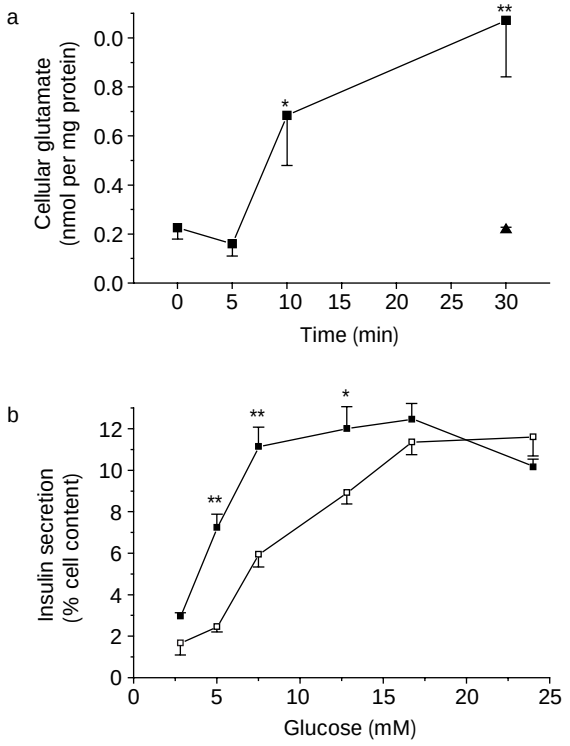

Figure 1 Glutamate production and effects of dimethylglutamate in INS-1 insulinoma cells. **a**, Changes in cellular glutamate levels during incubation of INS-1 cells in the presence of 2.8 mM (filled triangles) or 12.8 mM (filled squares) glucose. The results are means ±s.e.m., $n = 6$ independent experiments done in duplicate; $^*P < 0.05$, $^{**}P < 0.005$ versus $t = 0$. **b**, Dimethylglutamate (5 mM met-Glut, filled squares) sensitizes glucose-induced insulin secretion in INS-1 cells. Non-esterified, cell-impermeant glutamate does not enhance insulin secretion (data not shown). The results are means ±s.e.m., $n = 4$ of one out of three similar experiments; $^*P < 0.05$, $^{**}P < 0.005$ versus corresponding glucose control (open squares).

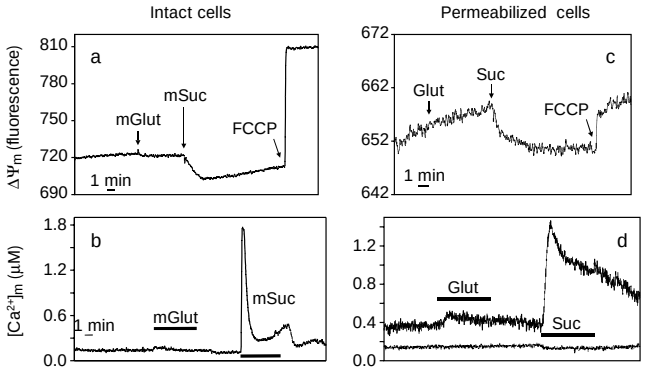

Figure 2 Mitochondrial membrane potential ($\Delta\Psi_m$) and $[Ca^{2+}]_m$ in intact and permeabilized INS-1 cells. **a**, **b**, Effects of cell-permeant dimethylester-L-glutamate (5 mM, mGlut) and monomethylester succinate (5 mM, mSuc) on $\Delta\Psi_m$ (**a**) and $[Ca^{2+}]_m$ (**b**). **c**, **d**, Effects of 1 mM L-glutamate (Glut) or 1 mM succinate (Suc) on $\Delta\Psi_m$ (**c**) and $[Ca^{2+}]_m$ (**d**) in α-toxin-permeabilized INS-1 cells incubated at 500 nM $[Ca^{2+}]_c$ (thin bottom line in **d** at 100 nM $[Ca^{2+}]_c$). In **a** and **c**, $\Delta\Psi_m$ is measured in a cuvette and mitochondria are finally maximally depolarized (upward deflection) with 1 μM of the protonophore FCCP. The traces are representative of 3–5 independent experiments.

remains a prerequisite for glutamate-induced activation of the exocytotic machinery. Accordingly, at basal 100 nM $[Ca^{2+}]_c$, glutamate failed to stimulate insulin secretion (Fig. 3c). As insulin exocytosis requires not only Ca^{2+} but also ATP[1], we next investigated the interactions of ATP and glutamate. Even when the ambient ATP was increased 10-fold to the saturating concentration of 10 mM (at 500 nM $[Ca^{2+}]_c$), insulin secretion (% cell content per 10 min) was stimulated from 5.29 ± 0.57 to 10.26 ± 2.29 by 1 mM glutamate ($P < 0.05$) compared with 11.58 ± 2.08 by 1 mM succinate ($P < 0.02$). Thus, ATP does not mediate the effect of glutamate on exocytosis.

We also monitored the changes in cytosolic [ATP] together with insulin secretion in the same permeabilized cells expressing the ATP sensor luciferase in the cytosol[15]. Activation of the mitochondrial respiratory chain, seen as hyperpolarization of $\Delta\Psi_m$, promotes the synthesis of ATP in mitochondria. Succinate (1 mM), which hyperpolarized the $\Delta\Psi_m$ (Fig. 2c), generated ATP (2.4-fold) in permeabilized cells perifused with basal 1 mM ATP and 500 nM $[Ca^{2+}]_c$ (Fig. 3d). Unexpectedly, 1 mM glutamate also increased cytosolic [ATP] (1.9-fold) (Fig. 3d), without activating the respiratory chain, as demonstrated by the lack of effect on $\Delta\Psi_m$ (Fig. 2c).

Monitoring of [ATP] in perifused permeabilized cells reflects the net cytosolic ATP concentration resulting from exogenous (buffer) and endogenous (mitochondria) ATP supplies balanced by ATP consumption owing to ATPase activity (mainly Ca^{2+}-ATPases). Inhibition of the mitochondrial ATP synthase[10] with oligomycin lowered basal cytosolic [ATP] but did not abolish the effect of glutamate (Fig. 4b). Moreover, the effect on insulin secretion was well preserved (Fig. 4a). Under these conditions, succinate did not increase cytosolic [ATP] or insulin exocytosis (data not shown). These results establish that the secretory response evoked by the addition of glutamate does not require mitochondrial metabolism and suggest a non-mitochondrial origin for the ATP augmented by glutamate.

Like chromaffin granules[16] and synaptic vesicles[17], insulin-containing granules[18,19] are acidic inside (pH ≈ 5.0). The pH gradient is generated by a proton pump (vacuolar-type H^+-ATPase) using cytosolic ATP[16,18]. As a consequence, a membrane potential is created which is positive inside[17,18,20]. The sum of the pH gradient and the membrane potential, the electrochemical proton gradient,

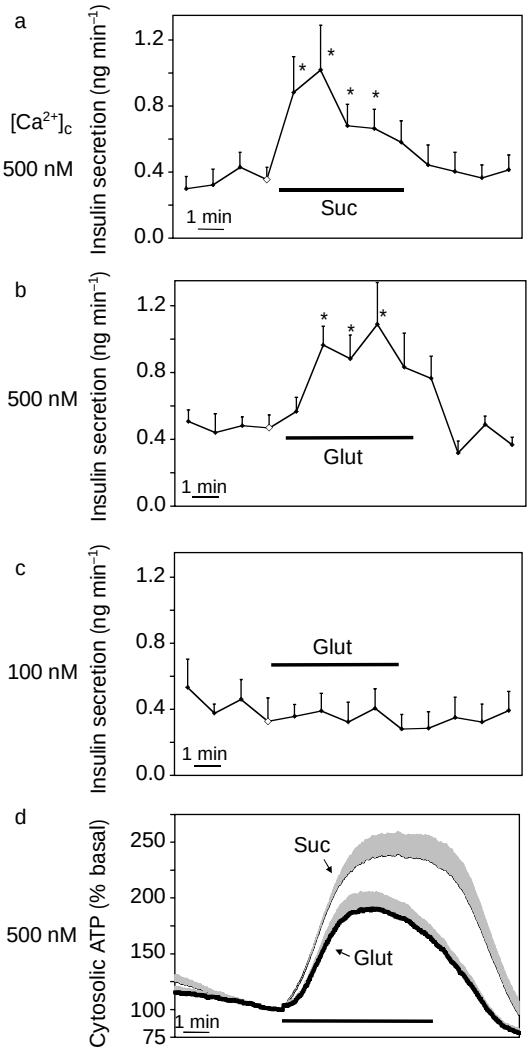

Figure 3 Effects of succinate and glutamate on insulin secretion and cytosolic [ATP] in α-toxin-permeabilized INS-1 cells. Cells are perifused at 500 nM (**a**, **b**, **d**) or 100 nM (**c**) free Ca^{2+} and 1 mM ATP. Insulin secretion is measured (**a–c**) in the effluent of cell preparations monitored for cytosolic [ATP] (**d**) through bioluminescence of cytosolic luciferase. Effects of: **a**, **d** (thin line), 1 mM succinate (Suc); **b**, **d** (thick line), 1 mM L-glutamate (Glut) at 500 nM $[Ca^{2+}]_c$; **c**, 1 mM Glut at 100 nM $[Ca^{2+}]_c$. The results are means ±s.e.m. (depicted by a shaded area for ATP), $n = 6$ (**a**, **d**), 7 (**b**, **d**) and 4 (**c**) independent experiments; in **a** and **b**, $^*P < 0.05$ versus the time point just preceding stimulation (open diamond).

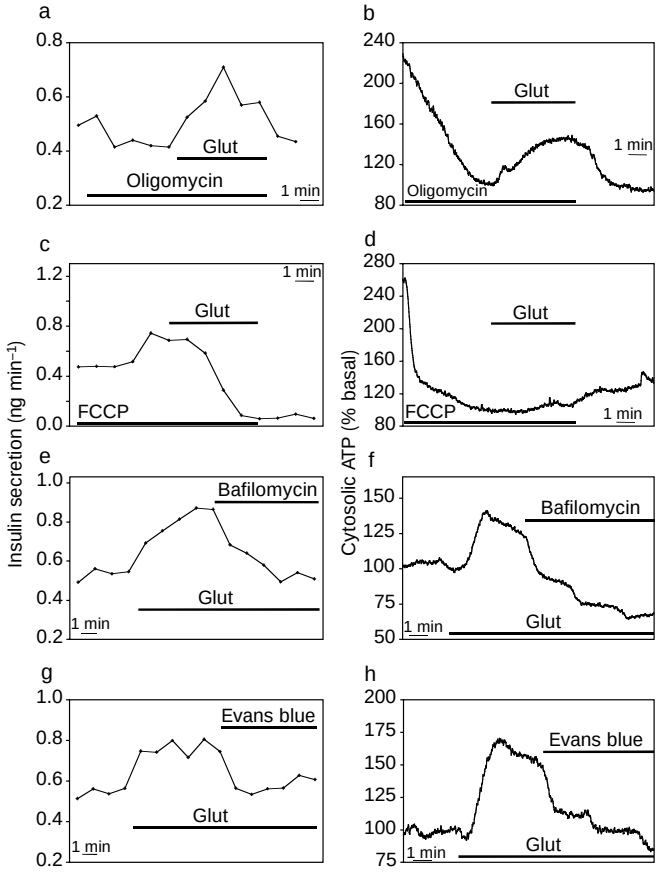

Figure 4 Effects of different inhibitors on the action of glutamate on insulin secretion (left) and cytosolic [ATP] (right) in permeabilized INS-1 cells. Cells are perifused at 500 nM Ca^{2+} and 1 mM ATP. Insulin secretion is measured in the effluent of the cell preparations monitored for cytosolic [ATP]. **a**, **b**, Effects of 1 mM L-glutamate (Glut) in the presence of 1 μg ml^{-1} of the mitochondrial ATP synthase inhibitor oligomycin. **c**, **d**, Effects of 1 mM Glut in the presence of 1 μM of the protonophore FCCP. **e**, **f**, Effects of 100 nM of the vacuolar-type H^+-ATPase inhibitor bafilomycin during stimulation with 1 mM Glut. **g**, **h**, Effects of 2 μM of the glutamate transport inhibitor Evans blue during stimulation with 1 mM Glut. The traces are representative of 3–5 independent experiments.

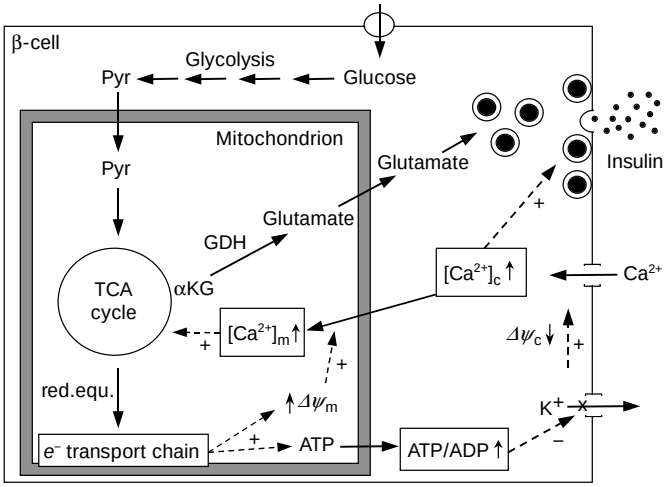

Figure 5 Proposed model for coupling glucose metabolism to insulin secretion in the β-cell. Glycolysis converts glucose to pyruvate (Pyr), which enters the mitochondrion and the TCA cycle resulting in the transfer of reducing equivalents (red. equ.) to the electron (e^-) transport chain, hyperpolarization of $\Delta\Psi_c$ and generation of ATP. Subsequently, closure of K_{ATP}-channels depolarizes $\Delta\Psi_c$ which opens voltage-senstive Ca^{2+} channels, raising $[Ca^{2+}]_c$ and triggering insulin exocytosis. At this time, under conditions of elevated $[Ca^{2+}]_c$, hyperpolarized $\Delta\Psi_m$ increases $[Ca^{2+}]_m$, further activating the TCA cycle. Glutamate is then formed from α-ketoglutarate (αKG) by the glutamate dehydrogenase (GDH). Glutamate uptake by granules leads to the second phase of insulin secretion.

drives glutamate uptake into the vesicular compartment via a specific transporter[17,21]. Dissipation of both the proton gradient and the vesicular membrane potential with protonophores[20] inhibits glutamate uptake[17,21]. Either FCCP or oligomycin can deplete ATP, but only FCCP affects the vesicular proton gradient, which is left intact by oligomycin. In the presence of FCCP, insulin release was transiently augmented, probably through a direct effect on the granules[21] and, thereafter, glutamate no longer increased insulin secretion and [ATP] (Fig. 4c, d). This indicates that glutamate uptake by the secretory granules is implicated in the elevation of cytosolic [ATP]. This could be explained by two mechanisms. First, glutamate acidifies vesicles[17,21] and may thereby reduce the consumption of ATP by the vacuolar-type H^+-ATPase. Second, it is possible that glutamate uptake promotes ATP production by reversal of the vacuolar-type H^+-ATPase[16,22]. The effect of glutamate on cytosolic [ATP] was abolished by specific inhibition of the vacuolar ATPase (Fig. 4f) or the vesicular glutamate transporter (Fig. 4h), further indicating the granules as the ATP source.

Bafilomycin (which blocks the vacuolar ATPase) and FCCP inhibit glutamate uptake by synaptic vesicles[23]. The abrogation of glutamate-induced insulin exocytosis observed with FCCP and bafilomycin (Fig. 4c, e) is probably secondary to blockage of glutamate uptake by the secretory granules. This notion was further substantiated by results obtained with Evans blue, a competitive inhibitor of the vesicular glutamate transporter[21,23]. Evans blue abolished the glutamate-induced insulin secretion (Fig. 4g), without affecting insulin release at basal conditions (500 nM Ca^{2+}) (not shown).

In the brain, glutamate is the primary extracellular messenger stored in synaptic vesicles[21]. We propose a novel role for glutamate as an intracellular messenger in insulin exocytosis. Glutamate uptake would render the insulin granules secretion competent. This could occur through the reduction of granular membrane potential[17] or, possibly, through Ca^{2+} uptake into the granules, as Ca^{2+} depletion of this compartment inhibits insulin exocytosis[24]. It is of interest in this context that Ca^{2+}-evoked exocytosis in permeabilized mast cells is strictly dependent on the presence of glutamate[25]. Glutamate uptake could also result in granule swelling, enabling the granule to fuse with the plasma membrane, a phenomenon described in zymogen granules[26]. The production of glutamate during glucose stimulation unravels an essential role for the mitochondria in exocytosis. Glutamate does not initiate the secretory response and its production from glucose requires Ca^{2+} entry into the cell and a rise in $[Ca^{2+}]_m$, which in turn increases the carbon flux through the TCA cycle[8,27]. The lag in glutamate generation (5–10 min; Fig. 1a) suggests that the molecule is implicated in the second, sustained phase of the biphasic glucose-induced insulin secretion[5].

Therefore, glutamate acts as an intracellular messenger in the normal regulation of insulin secretion in response to glucose (Fig. 5). It is noteworthy that children with mutations in the glutamate dehydrogenase gene, which results in excessive enzyme activity, display hypersecretion of insulin[28]. □

Methods

Cell culture

INS-1 cells were cultured in RPMI 1640 medium with 5% fetal calf serum (FCS) as previously described[7]. Stable clones of INS-1 cells expressing the Ca^{2+}-sensitive photoprotein aequorin targeted to the mitochondria (INS-1/EK3) were used to measure $[Ca^{2+}]_m$ (ref. 9). Clonal INS-1 lines expressing cytosolic luciferase (INS-r3-LUC7) were used for monitoring cytosolic [ATP] in living cells[15]. Human pancreatic islets were isolated by collagenase digestion and cultured free floating in CMRL-1066 medium with 10% FCS before the experiments[12].

Cellular glutamate determination

Attached INS-1 cells or free-floating human islets were cultured in 10-cm Petri dishes and preincubated for 2 h in glucose-free RPMI 1640 medium at 37 °C. Cells were then incubated for the indicated times at 37 °C in Krebs–Ringer bicarbonate HEPES buffer (KRBH) containing (in mM): 135 NaCl, 3.6 KCl, 10 HEPES (pH 7.4), 5 $NaHCO_3$, 0.5 NaH_2PO_4, 0.5 $MgCl_2$, 1.5 $CaCl_2$ and 2.8 glucose. The stimulatory glucose concentration was 12.8 mM for INS-1 cells and 16.7 mM for human islets. Stimulation was ended by putting the Petri dishes on ice and adding 1 ml of lysis buffer (20 mM Tris–HCl pH 8.0, 2 mM CDTA, 0.2% Tween-20) to the cells after discarding the incubation buffer. Following protein determination (Bradford's assay), glutamate levels were measured in cell homogenates by monitoring NADH fluorescence augmentation during oxidation of glutamate in the cell extracts in the presence of an excess of glutamate dehydrogenase (Boehringer-Mannheim) as described[29], with modifications. NADH fluorescence, excited at 340 nm, was measured at 460 nm in an LS-50B fluorimeter (Perkin-Elmer) before and after a 30-min incubation at room temperature in 1.5 ml buffer (50 mM Tris–HCl pH 9.5, 2.6 mM EDTA, 1.4 mM NAD, 1 mM ADP) and basal NADH was subtracted. Glutamate levels were corrected according to internal standards.

Cell permeabilization

Attached INS-1 cells were grown on coverslips coated with an extracellular matrix[8] and permeabilized after a 3–5 day culture period. Cells were first washed with a Ca^{2+}-free KRBH buffer before permeabilization with *Staphylococcus aureus* α-toxin (2.5 μg per coverslip, that is, per 4–5 × 10^5 cells) at 37 °C for 10 min in 100 μl of an intracellular-type buffer adjusted to approximately 100 nM free Ca^{2+} (140 mM KCl, 5 mM NaCl, 7 mM $MgSO_4$, 20 mM HEPES, pH 7.0, 1 mM ATP, 10.2 mM EGTA, 1.65 mM $CaCl_2$)[7]. Where mentioned, perifusion was done with the same low Ca^{2+} intracellular buffer or switched to 500 nM free Ca^{2+} concentration (140 mM KCl, 5 mM NaCl, 7 mM $MgSO_4$, 20 mM HEPES, pH 7.0, 10.2 mM EGTA, 6.67 mM $CaCl_2$) with 1 or 10 mM ATP as indicated[7].

Static insulin secretion

For static incubations, INS-1 cells were cultured for 3–5 days in complete RPMI 1640 medium. Before the experiments, cells were maintained for 2 h in glucose-free culture medium, washed and preincubated in glucose-free KRBH for 30 min and then incubated in the presence of the appropriate stimuli for 30 min at 37 °C. Insulin secretion and cellular insulin content extracted with acid–ethanol were determined by radioimmunoassay using rat insulin as a standard[7]. Static incubations of permeabilized cells were performed as previously described[7]. Where indicated, insulin release was measured in the effluent of permeabilized cells undergoing monitoring of luminescence (see next section). For all insulin secretion experiments, 0.1% of bovine serum albumin (Sigma) was added to buffers as carrier.

Mitochondrial membrane potential

The $\Delta\Psi_m$ was measured in a suspension of intact or α-toxin-permeabilized cells previously loaded with 10 μg ml^{-1} rhodamine-123. The fluorescence was excited at 490 nm and measured at 530 nm in an LS-50B fluorimeter at 37 °C in a cuvette with gentle stirring[7].

Measurements of luminescence and insulin secretion

Luciferase- or aequorin-expressing cells were seeded on coverslips 3–5 days before analysis. Before luminescence measurements, cells were maintained in glucose-free RPMI 1640 for 2 h at 37 °C. This period also served to load aequorin-expressing cells with 2.5 μM coelenterazine, the prosthetic group of aequorin[9]. Luminescence was measured in a thermostatted chamber at 37 °C by a photon detector connected to a photomultiplier apparatus (EMI 9789, Thorn-EMI) and data were collected each second on a computer photon-counting board (EMI C660)[9]. The cells were perifused constantly at a rate of 1 ml min^{-1} and, where indicated, fractions (one per min) were collected from the effluent for insulin measurement. Intact cells were perifused with KRBH and 10 μM beetle luciferin was added to the buffer for cytosolic [ATP] monitoring in luciferase-expressing cells[15].

Received 30 April; accepted 9 September 1999.

1. Wollheim, C. B., Lang, J. & Regazzi, R. The exocytotic process of insulin secretion and its regulation by Ca^{2+} and G-proteins. *Diabetes Rev.* **4,** 276–297 (1996).
2. Matschinsky, F. M. A lesson in metabolic regulation inspired by the glucokinase glucose sensor paradigm. *Diabetes* **45,** 223–241 (1996).
3. Ashcroft, F. M. *et al*. Stimulus-secretion coupling in pancreatic beta cells. *J. Cell Biochem.* **55,** 54–65 (1994).
4. Lang, J. Molecular mechanisms and regulation of insulin exocytosis as a paradigm of endocrine secretion. *Eur. J. Biochem.* **259,** 3–17 (1999).
5. Gembal, M., Gilon, P. & Henquin, J. C. Evidence that glucose can control insulin release independently from its action on ATP-sensitive K^+ channels in mouse B cells. *J. Clin. Invest.* **89,** 1288–1295 (1992).
6. Sato, Y., Aizawa, T., Komatsu, M., Okada, N. & Yamada, T. Dual functional role of membrane depolarization/Ca^{2+} influx in rat pancreatic B-cell. *Diabetes* **41,** 438–443 (1992).
7. Maechler, P., Kennedy, E. D., Pozzan, T. & Wollheim, C. B. Mitochondrial activation directly triggers the exocytosis of insulin in permeabilized pancreatic β-cells. *EMBO J.* **16,** 3833–3841 (1997).
8. Maechler, P., Kennedy, E. D., Wang, H. & Wollheim, C. B. Desensitization of mitochondrial Ca^{2+} and insulin secretion responses in the beta cell. *J. Biol. Chem.* **273,** 20770–20778 (1998).
9. Kennedy, E. D. *et al*. Glucose-stimulated insulin secretion correlates with changes in mitochondrial and cytosolic Ca^{2+} in aequorin-expressing INS-1 cells. *J. Clin. Invest.* **98,** 2524–2538 (1996).
10. Duchen, M. R. Contributions of mitochondria to animal physiology: from homeostatic sensor to calcium signalling and cell death. *J. Physiol. (Lond.)* **516,** 1–17 (1999).
11. Fisher, H. F. L-glutamate dehydrogenase from bovine liver. *Meth. Enzymol.* **113,** 16–27 (1985).
12. Janjic, D. *et al*. Improved insulin secretion of cryopreserved human islets by antioxidant treatment. *Pancreas* **13,** 166–172 (1996).
13. Sener, A. *et al*. Insulinotropic action of glutamic acid dimethyl ester. *Am. J. Physiol.* **267,** E573–E584 (1994).
14. Eto, K. *et al*. Role of NADH shuttle system in glucose-induced activation of mitochondrial metabolism and insulin secretion. *Science* **283,** 981–985 (1999).
15. Maechler, P., Wang, H. & Wollheim, C. B. Continuous monitoring of ATP levels in living insulin secreting cells expressing cytosolic firefly luciferase. *FEBS Lett.* **422,** 328–332 (1998).
16. Johnson, R. G. Jr Proton pumps and chemiosmotic coupling as a generalized mechanism for neurotransmitter and hormone transport. *Ann. N. Y. Acad. Sci.* **493,** 162–177 (1987).
17. Maycox, P. R., Deckwerth, T., Hell, J. W. & Jahn, R. Glutamate uptake by brain synaptic vesicles. Energy dependence of transport reconstitution in proteoliposomes. *J. Biol. Chem.* **263,** 15423–15428 (1988).
18. Hutton, J. C. The internal pH and membrane potential of the insulin-secretory granule. *Biochem. J.* **204,** 171–178 (1982).
19. Orci, L. *et al*. Conversion of proinsulin to insulin occurs coordinately with acidification of maturing secretory vesicles. *J. Cell Biol.* **103,** 2273–2281 (1986).
20. Breckenridge, L. J. & Almers, W. Currents through the fusion pore that forms during exocytosis of a secretory vesicle. *Nature* **328,** 814–817 (1987).
21. Ozkan, E. D. & Ueda, T. Glutamate transport and storage in synaptic vesicles. *Jpn. J. Pharmacol.* **77,** 1–10 (1998).
22. Roisin, M. P., Scherman, D. & Henry, J. P. Synthesis of ATP by an artificially imposed electrochemical proton gradient in chromaffin granule ghosts. *FEBS Lett.* **115,** 143–147 (1980).
23. Roseth, S., Fykse, E. M. & Fonnum, F. Uptake of L-glutamate into rat brain synaptic vesicles: effect of inhibitors that bind specifically to the glutamate transporter. *J. Neurochem.* **65,** 96–103 (1995).
24. Scheenen, W. J., Wollheim, C. B., Pozzan, T. & Fasolato, C. Ca^{2+} depletion from granules inhibits exocytosis. A study with insulin-secreting cells. *J. Biol. Chem.* **273,** 19002–19008 (1998).
25. Churcher, Y. & Gomperts, B. D. ATP-dependent and ATP-independent pathways of exocytosis revealed by interchanging glutamate and chloride as the major anion in permeabilized mast cells. *Cell Regul.* **1,** 337–346 (1990).
26. Jena, B. P. *et al*. G_i regulation of secretory vesicle swelling examined by atomic force microscopy. *Proc. Natl Acad. Sci. USA* **94,** 13317–13322 (1997).
27. Hyder, F. *et al*. Increased tricarboxylic acid cycle flux in rat brain during forepaw stimulation detected with $^1H[^{13}C]$NMR. *Proc. Natl Acad. Sci. USA* **93,** 7612–7617 (1996).
28. Stanley, C. A. *et al*. Hyperinsulinism and hyperammonemia in infants with regulatory mutations of the glutamate dehydrogenase gene. *N. Engl. J. Med.* **338,** 1352–1357 (1998).
29. Cho, S. W., Lee, J. & Choi, S. Y. Two soluble forms of glutamate dehydrogenase isoproteins from bovine brain. *Eur. J. Biochem.* **233,** 340–346 (1995).

Acknowledgements

We thank C. Bartley and G. Chaffard for technical assistance, J. Lou, J. Oberholzer and P. Morel (Department of Surgery, University Hospital of Geneva) for supplying human islets, A. Valeva (Institute of Medical Microbiology, University of Mainz) for α-toxin and T. Pozzan, P. Antinozzi and H. Ishihara for discussions. This study was supported by the Swiss National Science Foundation and the AETAS Foundation (Geneva).

Correspondence and requests for materials should be addressed to P.M. (e-mail: pierre.maechler@medecine.unige.ch).

The TOR signalling pathway controls nuclear localization of nutrient-regulated transcription factors

Thomas Beck & Michael N. Hall

Department of Biochemistry, Biozentrum, University of Basel, CH-4056 Basel, Switzerland

The rapamycin-sensitive TOR signalling pathway in *Saccharomyces cerevisiae* activates a cell-growth program in response to nutrients such as nitrogen and carbon[1–4]. The TOR1 and TOR2 kinases (TOR) control cytoplasmic protein synthesis and degradation through the conserved TAP42 protein[5–8]. Upon phosphorylation by TOR, TAP42 binds and possibly inhibits type 2A and type-2A-related phosphatases[6–8]; however, the mechanism by which TOR controls nuclear events such as global repression of starvation-specific transcription is unknown. Here we show that TOR prevents transcription of genes expressed upon nitrogen limitation by promoting the association of the GATA transcription factor GLN3 with the cytoplasmic protein URE2. The binding of GLN3 to URE2 requires TOR-dependent phosphorylation of GLN3. Phosphorylation and cytoplasmic retention of GLN3 are also dependent on the TOR effector TAP42, and are antagonized by the type-2A-related phosphatase SIT4. TOR inhibits expression of carbon-source-regulated genes by stimulating the binding of the transcriptional activators MSN2 and MSN4 to the cytoplasmic 14-3-3 protein BMH2. Thus, the TOR signalling pathway broadly controls nutrient metabolism by sequestering several transcription factors in the cytoplasm.

Nitrogen limitation activates the partially redundant GATA factors GLN3 and GAT1[9–11]. We investigated a role of TOR in GLN3- and GAT1-dependent transcription. Wild-type cells were grown in rich medium to early logarithmic phase, treated with

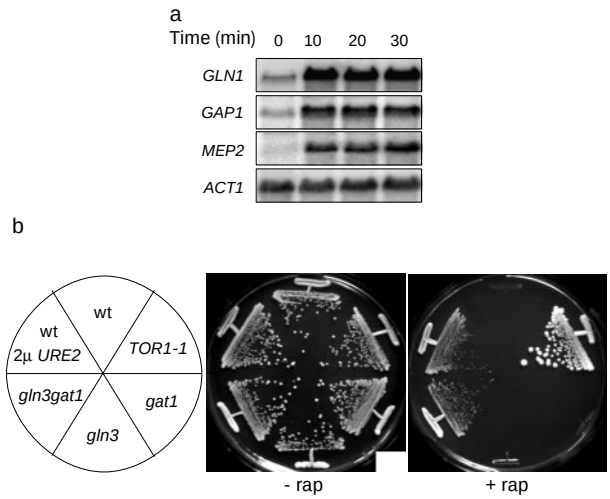

Figure 1 TOR inhibits the GATA transcription factors GLN3 and GAT1. **a**, Induction of GLN3- and GAT1-dependent transcription in response to TOR inactivation by rapamycin treatment. *GLN1*, *GAP1*, *MEP2* and *ACT1* transcripts from cells treated with rapamycin for the times indicated were probed. **b**, Overexpression of *URE2* or deletion of *GLN3* and *GAT1* confers rapamycin resistance. Growth of a wild-type strain overexpressing *URE2* (2 μ *URE2*; pTB376), strains deleted for *GLN3* (*gln3*), *GAT1* (*gat1*) or *GLN3* and *GAT1* (*gln3 gat1*), a wild-type (wt) strain and a rapamycin-resistant *TOR1-1* strain[14] on rich medium (–rap) and rich medium supplemented with 200 ng ml^{-1} of rapamycin (+rap) was compared. The –rap and +rap plates were incubated at 30 °C for 2 days and 5 days, respectively.